A Myosignal-Based Powered Exoskeleton System

Jacob Rosen, Moshe Brand, Moshe B. Fuchs, and Mircea Arcan

Abstract—Integrating humans and robotic machines into one system offers multiple opportunities for creating assistive technologies that can be used in biomedical, industrial, and aerospace applications. The scope of the present research is to study the integration of a human arm with a powered exoskeleton (orthotic device) and its experimental implementation in an elbow joint, naturally controlled by the human. The Human–Machine interface was set at the neuromuscular level, by using the neuromuscular signal (EMG) as the primary command signal for the exoskeleton system. The EMG signal along with the joint kinematics were fed into a myoprocessor (Hill-based muscle model) which in turn predicted the muscle moments on the elbow joint. The moment-based control system integrated myoprocessor moment prediction with feedback moments measured at the human arm/exoskeleton and external load/exoskeleton interfaces. The exoskeleton structure under study was a two-link, two-joint mechanism, corresponding to the arm limbs and joints, which was mechanically linked (worn) by the human operator. In the present setup the shoulder joint was kept fixed at given positions and the actuator was mounted on the exoskeleton elbow joint. The operator manipulated an external weight, located at the exoskeleton tip, while feeling a scaled-down version of the load. The remaining external load on the joint was carried by the exoskeleton actuator. Four indices of performance were used to define the quality of the human/machine integration and to evaluate the operational envelope of the system. Experimental tests have shown that synthesizing the processed EMG signals as command signals with the external-load/human-arm moment feedback, significantly improved the mechanical gain of the system, while maintaining natural human control of the system, relative to other control algorithms that used only position or contact forces. The results indicated the feasibility of an EMG-based power exoskeleton system as an integrated human–machine system using high- level neurological signals.

Index Terms—Arm, electromyography, EMG, exoskeleton, muscle, myosignals, orthotics, upper limb.

I. INTRODUCTION

INTEGRATING humans and robotic machines into one system offers multiple opportunities for creating new assistive technologies that can be used in biomedical, industrial, and aerospace applications. One of the human limits in performing physical tasks is the muscles' strength. In addition, muscle strength may be decreased substantially as a result of verity of neuromuscular diseases, muscular atrophy, and dystrophy in disabled people. As opposed to strength limitation, humans possess naturally developed algorithms with complex and highly specialized control methods, using higher and lower neural centers, that enable them to perform very complicated tasks such as locomotion while avoiding object collision. In contrast, robotic manipulators can perform tasks requiring large forces or moments, depending on the nature of their structure and on the power of their actuators. However, their artificial control algorithms which govern their dynamics miss the flexibility to perform in a wide rage of fuzzy conditions preserving the same quality of performance as humans. It seems therefore that combining these two entities, the human and the robot into one integrated system under the control of the human, may lead to a solution which will benefit from the advantages offered by each subsystem. The mechanical power of the machine integrated with the inherent human control system could perform tasks that need high forces in a very efficient manner. This is the underlying principle in the design of exoskeleton systems.

An exoskeleton is an external structural mechanism whose joints correspond to those of the human body. It is worn by the human and the physical contact between the operator and the exoskeleton allows direct transfer of mechanical power and information signals. The exoskeleton system can be used for three conceptually different applications:

1) power amplifier;
2) master device of a master/slave teleoperator system;
3) haptic device.

In utilizing the exoskeleton as a human power amplifier, the human provides control signals for the exoskeleton, while the exoskeleton actuators provide most of the power necessary for performing the task. The human becomes a part of the system and applies a scaled-down force compared with the load carried by the exoskeleton. For example, if the exoskeleton manipulates an object, the human may feel 10% of the load while the exoskeleton carries 90% of the load. Using the exoskeleton as a master device in a master/slave teleoperation system enables the operator attached to the exoskeleton (master) to control a robotic arm (slave). In a bilateral mode, the forces applied on the robotic arm by the environment are reflected back to the master and applied by the exoskeleton structure and actuators on the operator's arm. In this setup the operator feels the interaction between the robotic arm tool-tip and the environment (for a review see [1] and [2]). Employing the exoskeleton as a haptic device is a relatively new technology aimed to simulate human interaction with virtual object simulated in virtual reality. The operator is immersed in a virtual-realty environment wearing an exoskeleton. In that case a computer simulation is replacing the slave component and the realistic environment of the master/slave teleoperation with a virtual one. As a result,

a virtual object in that virtual environment can be touched by the operator, whereas the exoskeleton structure and its actuators provide a force feedback, emulating the real object including its mechanical and texture properties. The exoskeleton, in that sense, simulates an external environment and adds the sense of touch (haptics) to the graphical virtual environment (for a review see [1] and [3]–[5]). Several mechanisms including arms [6]–[13], hands [14], [15], and other haptic devices were developed for a wide range of applications.

Throughout the last three decades, several designs of exoskeleton, as a human powered amplifier, have been developed and evaluated. In studying the evolution of these systems two basic types with a different human machine interface (HMI) seem to emerge, which may be defined as generations. The first exoskeleton generation was developed based on a mission profile of the U.S. Department of Defense which defined the exoskeleton as a powered suite of armor to augment the lifting and carrying capabilities of soldiers. It was originally named man-amplifier. The primary intent was to develop a system that would greatly increase the strength of a human operator while maintaining human control of the manipulator. The first generation prototype known as the Hardyman was the first attempt to mechanically design a man-amplifying exoskeleton using a hydraulically powered articulated frame worn by an operator [16]–[20]. The Hardyman was comprised as a set of overlapping exoskeletons worn by a human operator. The master portion was the inner exoskeleton that was manipulated by the operator providing position command to the slave. The outer exoskeleton consisted of a hydraulically actuated slave, which followed all the motions of the master. Hardyman weighted 3300 Kg, had 30 degrees of freedom (DOF), and was designed for amplification ratio of 25 : 1. Crude by the standards of today, hydraulic sensors produced error signals from the inner exoskeleton to the outer exoskeleton. The biggest problem was the hydromechanical servo system employed in the legs. Unlike the arms, the legs needed constant coordination to achieve balance. Unsupported walking was not achieved [21].

The second generation of exoskeletons had the HMI at the dynamics level utilizing the direct contact forces between the human and the machine measured by force sensors as the main command signal to the exoskeleton. The human wore the extender, in a way that lumped them together mechanically. The operator was in full physical contact with the exoskeleton throughout its manipulation [22]–[25]. Several experimental extender prototypes were designed and built in order to study control issues.

A common feature in both the first and the second generation of exoskeletons was that the operator must apply an action, either kinematic-position command (first generation) or dynamic-contact force command (second generation), in order to trigger the exoskeleton response. Obviously, this sequence of events constitutes a source of delay in both systems.

The leading idea of current research is that setting the HMI at higher levels of the human physiological (neurological) system hierarchy allows us to overcome the electro-chemical–mechanical delay, which inherently exists in musculoskeletal system. This inherent time delay refers to the interval between the time

when the neural system activates the muscular system and the time when the muscles and the associate soft tissues contract mechanically and generate moments around the joints. During that time interval, the system will gather information regarding the muscle's neural activation level based on a processed neuromuscular (EMG) signals and the joint position and angular velocity. This information will be fed into a myoprocessor (muscle model) which will in turn predict the moment that is going to be developed by the physiological muscle relative to the joint. The main advantage of establishing the interface at the neuromuscular level is the ability to estimate the forces that will be generated by the muscles before the mechanical contractions actually occur. This information will be fed in to the exoskeleton system such that by the time the physiological muscles contract the exoskeleton amplifies the joint moment by a preselected gain factor. As a result, the reaction time of the human/machine system should decrease, resulting in a more natural control of the task. In line with this concept, a third generation of exoskeletons is proposed in the present study, setting the HMI at the human neuromuscular junction. The exoskeleton and the human are still mechanically linked with contact force sensors, as in the second generation apparatus. In this setup, however, the contact force sensors generate only feedback signals to correct the kinematics and the dynamics of the exoskeleton.

Studies have shown that the surface EMG recorded from bipolar electrodes during constant force (isotonic) constant-angle (isometric) nonfatiguing conditions can be modeled as a zero-mean correlation-ergodic, random process which is Gaussian distributed [26]–[28]. Under that conditions the EMG signal can be correlated to the torque developed by the muscles with respect to a joint [29], [30]. Processed EMG signals along with system identification models which noninvasively estimated muscle forces and joint torques have been used as the control input to myoelectrically controlled prostheses [31]–[35]. In operating a myoelectrically controlled powered prostheses the human neural control system and the prostheses control system are separate entities. The human operator provides command signals in a feed-forward open-loop fashion utilizing only visual feedback as the primary source of information while maintaining a direct line of sight when attempting to grasp or place an object [36]. Feedback information based on visual and auditory cues is slower, less automated, and less programmed than the normal feedback [37]. As opposed to controlling a myoelectrically powered prostheses, in operating a myoelectrically powered exoskeleton (orthotic device) the human and the exoskeleton are mechanically linked, and therefore the human neural control system and exoskeleton control system coexist and have to cooperate by sharing the same kinematics and dynamics constraints. Moreover, when an exoskeleton is used, the nonisometric and nonisotonic conditions, which are valid assumption for controlling a prosthetic devise using EMG signals alone, do not hold, and therefore the muscle's force cannot be estimated solely on the EMG signals. This is because the angle of the human limb joint, coupled with the exoskeleton joint, is constantly changing during the exoskeleton operation, and as a result the muscles attached to that joint are changing their length and end points velocities. Therefore, the muscle model (myoprocessor) has to

take into account the muscle's length and velocity in addition to the EMG signal, that defines the muscle activation level, for predicting the force that will be developed by the physiological muscle.

In order to establish an interface at the neuromuscular junction, two basic conditions have to be fulfilled. The first condition is the capability to measure the biosignals. In the present study the myosignals of the muscles involved in the elbow flexion/extension movement are measured by surface electrodes, using noninvasive techniques. The second condition is the ability to simulate and to predict the functions of the human body subsystems and organs from the interface level (myosignals) down to the lower levels of the physiological hierarchy (skeletal muscle forces and moments). The term myoprocessor [38] was used to define the component of the system that simulates the human skeletal muscle behavior and provides an estimation of the muscle forces. The present implementation uses a Hill-based muscle model although in a previous work neural network models were also studied [39].

The main purpose of the powered exoskeleton system is to amplify the load carrying capacity of a healthy operator; however, it can also be used as an upper limb orthosis for physically impaired humans [36]. For a patient to employ any powered exoskeleton, he or she must have some minimal motor control abilities in order to generate neural signals. The powered exoskeleton improves the patient's limb performance while utilizing what remains from the natural motor control functions of the operator. Thus, instead of promoting muscle atrophy, this powered exoskeleton system could be therapeutic by enhancing further muscle development, due to resurgence of limb use.

In the following sections the powered exoskeleton system for the elbow joint and its experimental implementation were described. The apparatus, in conjunction with appropriate control algorithm, was designed, built, and operated using high level HMI-EMG signals. The experimental system's overall performance envelope was studied followed by conclusions as well as an outline of anticipated future research.

II. METHOD— SYSTEM AND ITS EXPERIMENTAL PROTOCOLS
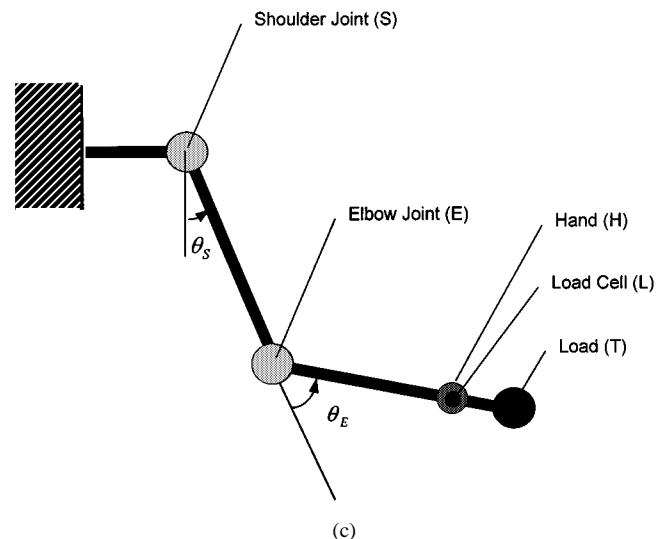
A. Experimental System

The experimental exoskeleton structure is shown in Fig. 1. It consisted of a two-link, two-joint mechanism corresponding to the upper and the lower arm and to the shoulder and elbow joints of the human body. The system included a weight plate (external load) that can be attached to the tip of the exoskeleton forearm link. The mechanism was fixed to the wall and positioned parallel to the sagittal plane of the operator. The human/exoskeleton mechanical interface included the upper arm bracelet, located at the upper arm link, and a handle grasped by the operator. This two-joint mechanism was used as a 1 DOF system by fixing the system shoulder joint (θ_S) at specific angles in the range of 0°–180°. The elbow joint (θ_E) was free to move in an angle range of 0°–145° and included built-in mechanical constraints which kept the exoskeleton joint angle within the average human anthropometric boundaries. Since the human arm and the exoskeleton were mechanically
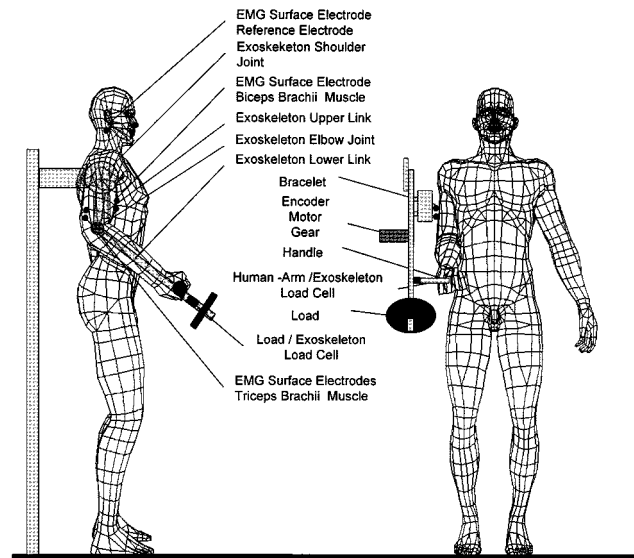
(a)
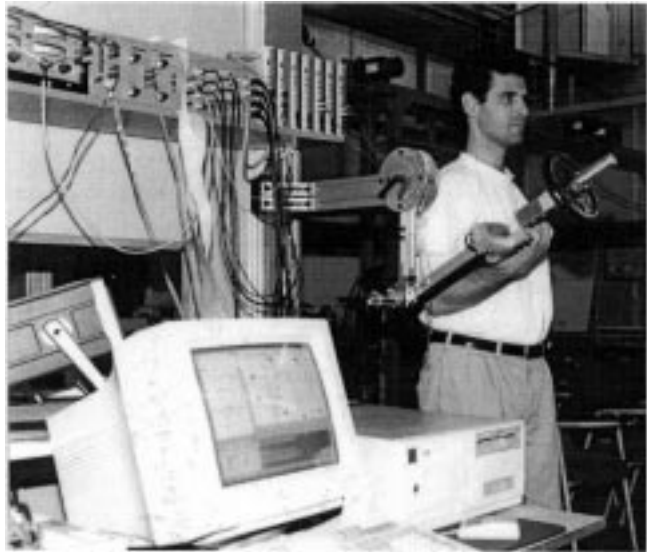
(b)

(c)

Fig. 1. Exoskeleton experimental system. (a) Schematic overview. (b) System overview (c) System components.
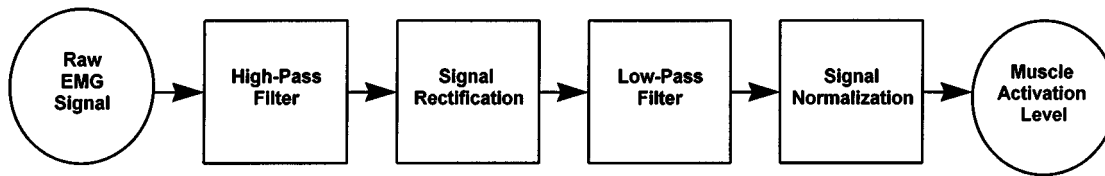
Fig. 2.   EMG signal processing algorithm for estimating the muscle activation level—block diagram.

linked the movements of the forearms of both the human and the exoskeleton were identical.

The basic purpose of the exoskeleton system as an assistive device is to amplify the moment generated by the human muscles relative to the elbow joint, while manipulating loads. The exoskeleton's elbow joint was powered by a dc servo motor (ESCAP-35NT2R82) with a stall torque of 360 Nm equipped with a planetary gearbox (ESCAP-R40) with a gear ratio of 1 : 193 and a maximal output torque of 40 Nm. An optical incremental shaft encoder (HP HEDS 5500) with 500 lines was attached to the motor shaft. Due to the encoder location and the high gear ratio, the practical encoder's resolution for measuring the joint angle was $0.0036°$. This setup incorporated a dc motor with the highest torque-to-weight ratio that was available on the commercial market at that time with a power consumption that could be provided by a battery. A high energy density of the power supply and an actuator with a high torque-to-weight ratio are two key features of the exoskeleton system as a self contained mobile medical assistive device for the disabled community. Limits imposed by present technology on these two key components along with design requirements for developing a compact system with a potential of serving as a medical assistive device for disabled person restricted the payload to be 5 kg. However, this biomedical oriented design does not restrict the generality of the exoskeleton concept or its operational algorithms. Using other actuation systems, like hydraulic system increases the load capacity substantially [22]–[25].

The exoskeleton forearm was extended by a rod with a special connector for attaching disk-type weights (external load). Two force sensors (TEDEA 1040) were mounted at the interfaces between the exoskeleton and the tip carrying the external load and between the exoskeleton and the human hand. The first load cell, inserted between the rod holding the external load and the exoskeleton forearm link, measured the actual shear force, normal to the forearm axis, applied by the external load. The second load cell was installed between the handle grasped by the human hand and the forearm link of the exoskeleton. This load cell measured the shear force applied by the operator to the handle. Multiplying the sensors' measurements by the corresponding moment arms indicated the moments applied by the weights and by the human hand relative the elbow joint.

Surface EMG electrodes (8 mm Ag–AgCl BIOPAC-EL208S) were attached to the subject's skin by adhesive disks at locations recommended in [40] for measuring the EMG signal of the *Biceps Brachii* and *Triceps Brachii* medial-head muscles. The signals were gained by EMG amplifiers (BIOPAC-EMG100A) using a gain factor in the range of 2000-5000 (depending on the subject). The EMG signals and the load cell signal were acquired by an A/D convector (Scientific Solution Lab Master 12

bit internal PC card) with a 1 kHz sampling rate, whereas the encoder signals were counted by custom-made hardware. The entire data set was recorded simultaneously and stored, for later off-line analysis and simulation.

A special real-time software, for operating the system, was written in C and run on a PC-based platform. The software was composed of three main modules. The first module dealt with the hardware/software interface. It controlled the interaction between the PC and the external motor driver and the sensors, through a D/A and an A/D card. The second module included the automatic code generated by the MATLAB-Simulink Real-Time toolbox. The third module was the user interface module which allowed to set various run time operational parameters. All the modules were compiled and linked for generating an efficient real-time software.

B. EMG Signal Processing and the Muscle Model

The human elbow joint complex can be considered as a 2 DOF joint including flexion–extension and pronation–supination joint movements. The exoskeleton, in its current mode, supported only the flexion–extension movement of the elbow joint. These movements are enabled by two sets of muscle groups: 1) the primary flexor muscles—the *Brachialis*, the *Biceps Brachii*, and the *Brachoradialis* and 2) the primary extensor muscle—*Triceps Brachii*. Out of the three flexor muscles the *Brachialis* has been referred to as a flexor par excellence of the elbow [41], [42]. Due to the fact that it is almost impossible to measure the EMG signals of the *Brachialis* by noninvasive techniques, the *Biceps Brachii* muscle was selected to represent the activation level of the joint flexor muscles group. As opposed to the elbow flexion movement that is preformed by three different muscles, the main elbow extension muscle is the *Triceps Brachii* that composed of three separate heads. The medial head is always active and appears to be the prime extensor of the elbow whereas the lateral and long heads act in reserve [42]. Based on this finding the *Triceps Brachii* medial-head was selected to represent the activation level of the joint extensor muscle group.

The algorithm for estimating the normalized muscle activation level (NAL), based on raw EMG signals, follows the signal processing procedure summarized in Fig. 2. It includes

1) a high-pass filter;
2) full signal rectification (absolute value);
3) a lowpass;
4) a signal normalization with respect to the EMG mean signal during maximal voluntary isometric contraction.

This algorithm is mapping the raw EMG signal with an arbitrary amplitude into a normalized signal in the range of $\langle 0, 1 \rangle$, where
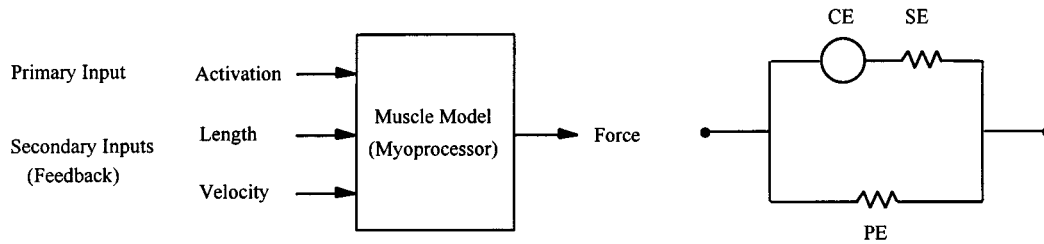
Fig. 3.   Hill-type muscle model—block diagram.

a value of 1 stands for maximal voluntary muscle activation. The NAL, in conjunction with the joint kinematics, serve as inputs to the muscle model (myoprocessor) representing the muscle activation level of the muscle groups.

The key element of the myosignal based exoskeleton as a powered assistive device enabling the HMI at the neural level was the myoprocessor. This module predicted the elbow moments that would be developed by the physiological muscles. This prediction was then used as a primary command signal to the exoskeleton control system, which in turn operated the actuator, mounted on the exoskeleton elbow joint, to add its part of the moment developed at the elbow joint.

The myoprocessor which was implemented in the present work was a Hill-based (HB) muscle model whose inception dates back to the classical paper of Hill [43]. HB models are almost universally accepted in bioengineering as an appropriate mathematical representation of muscle mechanics, for studying the dynamics and control of movement [44]. In the context of this research, the HB myoprocessors were developed for the flexor and the extensor muscle groups separately predicting the moment (M_i) applied on the elbow joint by each one of these muscle groups. The muscles' net moment (M_{net}) was then the sum of its components with the corresponding [+] sign for agonist muscles and [−] sign for antagonist muscles

$$M_{net} = \sum_{1}^{n} M_i \qquad (1)$$

where n is the number of muscles activating the joint.

Although many researchers have contributed to the development of the Hill models, this study was based on its modern engineering version [45]–[50]. All physiological parameters were taken from these publications. The selection of this model was motivated by its successful implementation in multijoint neuromuscular systems, using practical muscle parameters.

A HB muscle model consists of three elements:

1) a contractile element (CE) which represents the force generated by the active muscle fibers using the muscle chemical energy;
2) a series element (SE) which models the mechanical response of muscle to rapid length changes
3) a parallel element (PE) which simulates the passive resistance of muscle to stretch generated by the passive soft connective tissue, including the tendon and the nonactive muscle fibers (Fig. 3).

The only modification made to the Winters' formulation [45]–[50] included a generalized, continuous, dimensionless form of the CE force–velocity characteristics which synthesized both the shortening and the lengthening phases in one mathematical equation. This form was initially proposed in [51] and further used in [52].

The myoprocessor algorithm, which solved the HB state equation, implemented the direct modeling approach, in which the inputs were the muscle activation levels (U_i) and joint kinematics (θ_E, $\dot{\theta}_E$), and the output was the muscle moment (M_i).

$$M_i = M_i(U_i, \theta_E, \dot{\theta}_E) \qquad i = 1, 2. \qquad (2)$$

As indicated previously, the *Biceps Brachii* was used as the flexor muscle ($i = 1$) and the *Triceps Bracii* medial head as the extensor muscle ($i = 2$). The CE-SE, 2 DOF complex employed the muscle activation level (U_i) and the joint angle (θ_E) as inputs to generate the active part of the total muscle moment. When solving the equations it was assumed, based on the model setup, that the moment of the CE was equal to the moment of the SE. The PE component of the model used the joint angle (θ_E) as input and generated the passive part of the muscle moment. The total muscle moment (M_i) was then the sum of its active and passive parts.

C. Control Algorithm

The exoskeleton complex is composed of two subsystems: the human and the exoskeleton. The task of the control algorithm is to achieve a natural integration between these two major components. This task is performed by the operator while preserving a constant mechanical gain in which the operator feels a scaled down version of the load. A full contact is maintained between the operator and the exoskeleton throughout the whole process.

A block diagram of the system components is shown in Fig. 4. The primary input to the system was the EMG signals of the elbow flexion/extension muscles group. These raw EMG signals were processed for evaluating the muscle normalized activation level. This muscle activation level, in conjunction with the joint kinematics, were next fed into the myoprocessor (Hill-based muscle model) which produced an estimation of the moment to be generated by the muscles on the elbow joint. This constituted the primary input to the controller. The controller's inner closed loop (feedback signals) was composed from two sources: 1) the external-load/exoskeleton load cell, measuring the effective moment applied by the load to the elbow joint, and 2) the human-arm/exoskeleton load cell which monitored the moment applied by the operator on the system. After processing all this
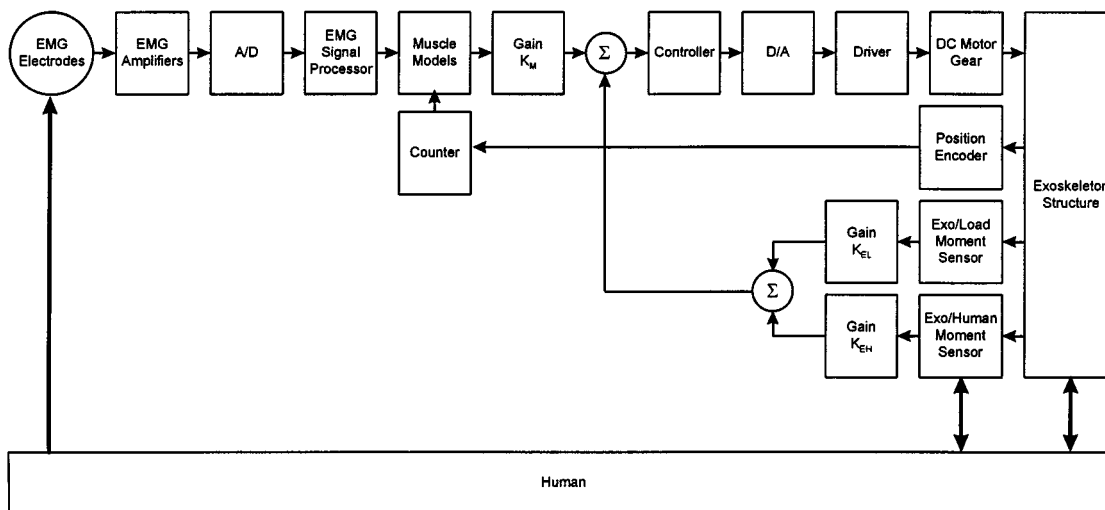
Fig. 4.   Exoskeleton system—component and signal flow diagram (command signal gain—muscle model gain K_M, feedback signal gain (load moment gain—K_{EL}, human-arm moment gain—K_{EH}).

information the controller generated a command signal to the dc motor driver.

From the system perspective, the control algorithm used three sets of feedback information (Fig. 4):

1) dynamic feedback—the moments generated at the interfaces between the human arm, the external load, and the exoskeleton structure;
2) kinematic feedback—the elbow joint angle measured by an encoder (the angular velocity and the angular acceleration were calculated by finite differences and filtered by a Butterworth fourth-order digital filter with a cutoff frequency of 10 Hz at 3 dB). These signals were used by the myoprocessor;
3) physiological feedback—the operator used his/her inherent biosensors and receptors (high level feedback—visualization, low level feedback—muscle spindle, tendon organ, joint receptors).

This physiological feedback was not implemented directly in the exoskeleton control scheme. However, it was taken into consideration by matching the exoskeleton controller frequency bandwidth to the human operator frequency bandwidth.

The control algorithm, based on a moment controller, was motivated by two leading ideas: 1) in operating the exoskeleton, the output of the myoprocessor (muscle model), used as the reference signal, was a moment command, and 2) for dc servo motor, the command to the linear driver, which in turn generates a current signal output, was directly proportional to the motor torque in the operational working range.

D. Experimental Protocol

The general characteristic of the arm movement that was used as part of the experimental protocol was full flexion/extension of the elbow during stationary positions of the shoulder joint. The forearm in full supination position was free to move in the two-dimensional (2-D) sagittal plane of the elbow joint ($0° \leq \theta_E \leq 145°$). The upper arm was constrained in a vertical position ($\theta_S = 0°$) so that the shoulder joint remained fixed

throughout the forearm movement. An experimental session consisted in moving the forearm, starting from full elbow joint extension ($\theta_E = 0°$), followed by full elbow joint flexion ($\theta_E = 145°$), and ended in the starting position ($\theta_E = 0°$). This movement was repeated four times in each experimental session. The forearm movement was performed while carrying weight plates of 2.5 kg connected to the exoskeleton tip (free end) at H. Resting periods of 5 min between each experimental session were imposed in order to avoid any fatigue effects.

The overall gain of the exoskeleton system can be adjusted by two sets of parameters (Fig. 4): 1) Command signal gain—muscle model gain K_M, 2) feedback signal gain (load moment gain—K_{EL}, human-arm moment gain—K_{EH}). In each set, the final output was the difference between the two channels. This difference was related to the net effect on the joint. For each channel, the gain parameter can be adjusted separately. In the case of the muscle model, based on the EMG signals, the input command was the difference between the muscle models (flexor/extensor) moment predictions (based on the activation levels of the *Biceps Brachii* and the *Triceps Brachii* and the joint kinematics). Using different gain levels for each channel allowed to determine the influence of each muscle on the total input command signal. From a physiological perspective, the maximal moment, generated by the muscles during flexion was higher than during extension. Selecting a higher EMG gain parameter for *Triceps Brachii* muscle, relative the *Biceps Brachii* muscle, enables to increase artificially the moments, generated during flexion, and in this way to equalize the exoskeleton flexion/extension movement.

In the case of the moment signal, the input feedback signal was the difference between the moment generated by the external load and the moment applied by the human arm. Each one of the channels was gained separately. The ratio between the gain factors of the load moment signal and the human arm moment signal determined the amplification factor of the human moment.

The overall performance of the exoskeleton system was studied experimentally using a gain mapping. The experimental

protocol included 93 experimental sessions. Each session consisted of four elbow joint flexion/extension movements of the forearm, maintaining the upper arm in a vertical position. This protocol was repeated for different sets of command signal gain (EMG) and feedback signal gain (Moment). The ratio between the EMG channels remained constant (the ratio between the *Biceps Brachii* muscle activation gain and the *Triceps Brachii* muscle activation gain was set to 1/8) and the same total gain (K_M—Fig. 4) was applied to both the *Biceps Brachii* and *Triceps Brachii* EMG signals (K_M—0, 0.5, 1, 1.5, 2, 2.5). On the other hand, different gain ratios were used for the human and load moment signals (K_{EL}/K_{EH}—0/0, 5/1 10/1, 15/1, 20/1 25/1, 30/1, 35/1, 40/1, 45/1, 50/1, 55/1, 60/1, 65/1, 70/1, 75/1, 80/1, 85/1, 90/1, 95/1 100/1—Fig. 4).

E. Performance Indices

Evaluating the overall performance of the exoskeleton is a multidimensional issue involving both subjective and objective criteria. The following four objective indices focused the evaluation process on the enhanced gain capability of the exoskeleton and on the way the enhanced gain was influencing the muscles activation. These performance indices included:

1) human arm moment and load moment;
2) mechanical moment gain;
3) mechanical work ratio;
4) muscles activation ratio.

1) Human Arm Moment and Load Moment Index: The primary index of the exoskeleton operation was based on the graph of the moment applied by the load on the exoskeleton during maneuvering an object as a function of the moment applied by the human arm (Fig. 5). This graph was divided into two regions marked by black color and gray color. In equal scaled axes (human arm moment axis and load moment axis) the lines inclined at 45° relative to the horizontal axis defined a state in which the load moment was equal to the human arm moment, a situation which existed when the exoskeleton motor was disconnected. The gray areas represented cases in which the human arm moment was lower than the load moment. Points in that region indicated states in which the exoskeleton increased the human arm moment. The difference between the load moment and the human arm moment was developed by the exoskeleton motor. In general, the gray area defined the desired operational regions. On the other hand, the black region indicated states in which the load moment was greater than the human arm moment. Those operational regions must be avoided since the exoskeleton is misused as a powered assistive device by artificially increasing the external load moment. Plotting the human arm moments as a function of the load moment on the moment map (Fig. 5) could lead to an amorphous shape on that map. However, a straight line indicated a constant gain throughout the exoskeleton operation.

2) Mechanical Moment Gain Index: The average mechanical gain was defined as the ratio between the moment applied by the load and the moment applied by the human arm on the exoskeleton as shown in (3). The design goal was to generate a constant gain factor. In the gain map [Fig. 5] a constant gain was defined by the slope of the straight line indicating a linear rela-
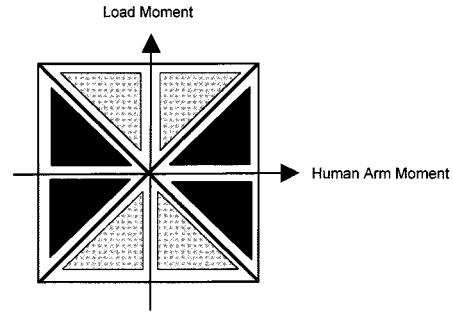

Fig. 5. Moment map—load moment applied on the exoskeleton during manipulating an object as a function of the human arm moment. Gray area—proper operational regions. Black area—nonproper operational regions.

tion between the load moment and the moment applied by the human. In practice, the mechanical moment gain was calculated based on the experimental data using linear least square algorithm (linear regression) of a graph plotted on a moment map. Mechanical moment gain index with a value of four ($G_M = 4$) practically indicated that 20% of the load was carried by the human arm and 80% of the load was supported by the exoskeleton structure/actuator.

$$G_M = \frac{M_L}{M_A} \tag{3}$$

where

M_A moment applied on the exoskeleton by the human arm;
M_L moment applied on the exoskeleton by the load;
G_M mechanical moment gain.

3) Mechanical Work Ratio Index: The mechanical work ratio was defined as the ratio between the work done by the human arm, manipulating the load, with and without the exoskeleton assistive (4). The mechanical work was calculated as the integral of the moment applied by the human arm relative to the elbow joint along the angular path of the forearm.

$$G_W = \frac{W_{HE}}{W_H} \tag{4}$$

where

W_{HE} mechanical work done by the human using the exoskelelton during load manipulation;
W_H mechanical work done by the human during load manipulation;
G_W mechanical work ratio.

4) Muscles' Activation Ratio: The muscles' activation ratio was defined as the ratio between the muscles' activation during manipulation of the load with and without the exoskeleton assistive (5). The muscle activation level, as a function of time, was estimated by the algorithm defined in Section II-B. The *Biceps Brachii* and the *Triceps Brachii* muscles were both, among others, activated and coactivated during the flexion/extension movement of the forearm. An index for the activation level, which was related to the effective net activity, is defined in (5). On the other hand, an index for the coactvation level, which identified the joint stiffness, was formulated in (6) and (7).

$$G_A = \frac{A_{HE}}{A_H} \tag{5}$$

where

A_{HE} muscle activation index of the human using the exoskelelton during load manipulation;

A_H muscle activation index of the human during load manipulation;

G_A muscle activation ratio.

$$A_A = \int_0^t u_{Bic}(t) + u_{Tri}(t)\, dt \tag{6}$$

$$A_C = \int_0^t |u_{Bic}(t) - u_{Tri}(t)|\, dt \tag{7}$$

where

A_A activation index;

A_C coactivation index;

t time;

u_{Bic} *Biceps Brachii* muscle activation;

u_{Bic} *Triceps Brachii* muscle activation.

The index which synthesizes both the muscles' activation (6) and coactivation (7) into one index is defined in (9) based on (8).

$$(u_{Bic} + u_{Tri})^2 + (u_{Bic} - u_{Tri})^2 = 2(u_{Bic}^2 + u_{Tri}^2) \tag{8}$$

$$A_H = \int_0^t u_{Bic}^2(t) + u_{Tri}^2(t)\, dt \tag{9}$$

where A_H = the total net activation index of the flexion/extension muscles.

III. RESULTS

The experiments described in this section were performed according to the experimental protocol defined in Section II-D. Typical experimental results are plotted in Fig. 6 showing the exoskeleton performance while manipulating a weight in two cases: 1) passive mode—the actuator (dc motor) is disconnected and the exoskeleton is used for measuring kinematic and dynamic data of a natural maneuvering the weight—Figs. 6(a)–(c) 2) active mode—the actuator is connected and the exoskeleton operates as an assistive device—Figs. 6(d)–(f).

The raw EMG signal and the muscle activation level are plotted in Figs. 6(a) and 6(d). Each plot represents the activity of two muscles: *Biceps Brachii* (BIC)—flexor muscle, and *Triceps Brachii* medial head (TRI)—extensor muscle. For each muscle, both the raw EMG signal and the muscle activation level, estimated according to the algorithm defined in Section II-B, are plotted for the passive and active mode. During the movement specified in the experimental protocol, the BIC was much more active in both the flexion/extension movements relative to the TRI. The two-phase peaks in the EMG data corresponded to the two phase peaks of the moment relative to the elbow joint [Figs. 6(c) and 6(f)]. The TRI activity was significant only at the end of the elbow full flexion aimed to overcome the passive stiffness of the flexor muscles. It is clear that the muscles' activation levels are drastically reduced in the active mode [Fig. 6(d)] relative to the passive mode [Fig. 6(a)],

a fact which emphasizes the contribution of the exoskeleton as an assistive device.

The kinematics data, namely the elbow joint angle, angular velocity, and angular acceleration are plotted in Figs. 6(b) and 6(e). The kinematics data indicated smooth and stable operation in the active mode [Fig. 6(e)] comparing to the passive (natural) mode [Fig. 6(b)]. The dynamic data define the moment applied by the load and the moment applied by the human arm on the exoskeleton, relative to the elbow joint, appears in Figs. 6(c) and 6(f) for passive and active modes of the exoskeleton, respectively. The elbow joint moment shape developed during the forearm movement was characterized by two peaks shape with a local minimum. The maximal values were developed when the forearm was at a position of 90° relative to the upper arm. The local minimum was generated during full flexion position, when the relative angle between the upper arm and the forearm was 145°. In the passive mode, the moment applied by the load and the arm should have the same value [Fig. 6(c)]. The mismatch between the moments, in a passive mode, was due to inertial effects that were applied, but not measured by the external load force sensor, as a results of its location at the exoskeleton forearm link tip, e.g., exoskeleton forearm internal torque, motor shaft inertial torque, and the gear friction torque). In the active mode, the moment applied, by the load, remained the same but the moment applied by the hand was significantly reduced [Fig. 6(f)]. The difference between the load moment and the hand moment was the moment developed by the exoskeleton actuator such that the operator sensed only a scaled-down version of the external load.

The human arm/powered exoskeleton natural integration was evaluated by comparing the moments developed while maneuvering an object with and without the assistance of the exoskeleton motor using the same experimental protocol defined previously. This comparison was done on the basis of the moment index performance (Fig. 7). Each point on the moment map is related to a forearm position or elbow joint angle at specific time intervals. A typical moment map with the corresponding human arm position during manipulating a load with the exoskeleton is shown in Fig. 7(a). The slope of the straight line indicates the average gain obtained by using the exoskeleton system.

Fig. 7(b) presents an experimental moment map. The graphs denoted by G_{ME6} and G_{ME1} depicted the moments of the load and the human arm when operating the exoskeleton with and without the assistance of the motor, respectively. The graph denoted by G_{ME1} defined the moments developed during a natural object manipulation. It was characterized by two branches. The lower branch, in which the external load moment was lower than the arm moment, was generated during movement against the gravity direction (in the present experimental setup-elbow flexion), whereas the upper branch, in which the load moment was higher than the arm moment, was generated by a movement along the gravity direction (in the present experimental setup-elbow extension). The gain of the overall movement was defined as 1, since the moment generated by the human arm must be equal to the inertial and gravity moments generated by the load. The graph denoted by G_{ME6} defined the moments developed during load manipulation with the assistance of the ex-
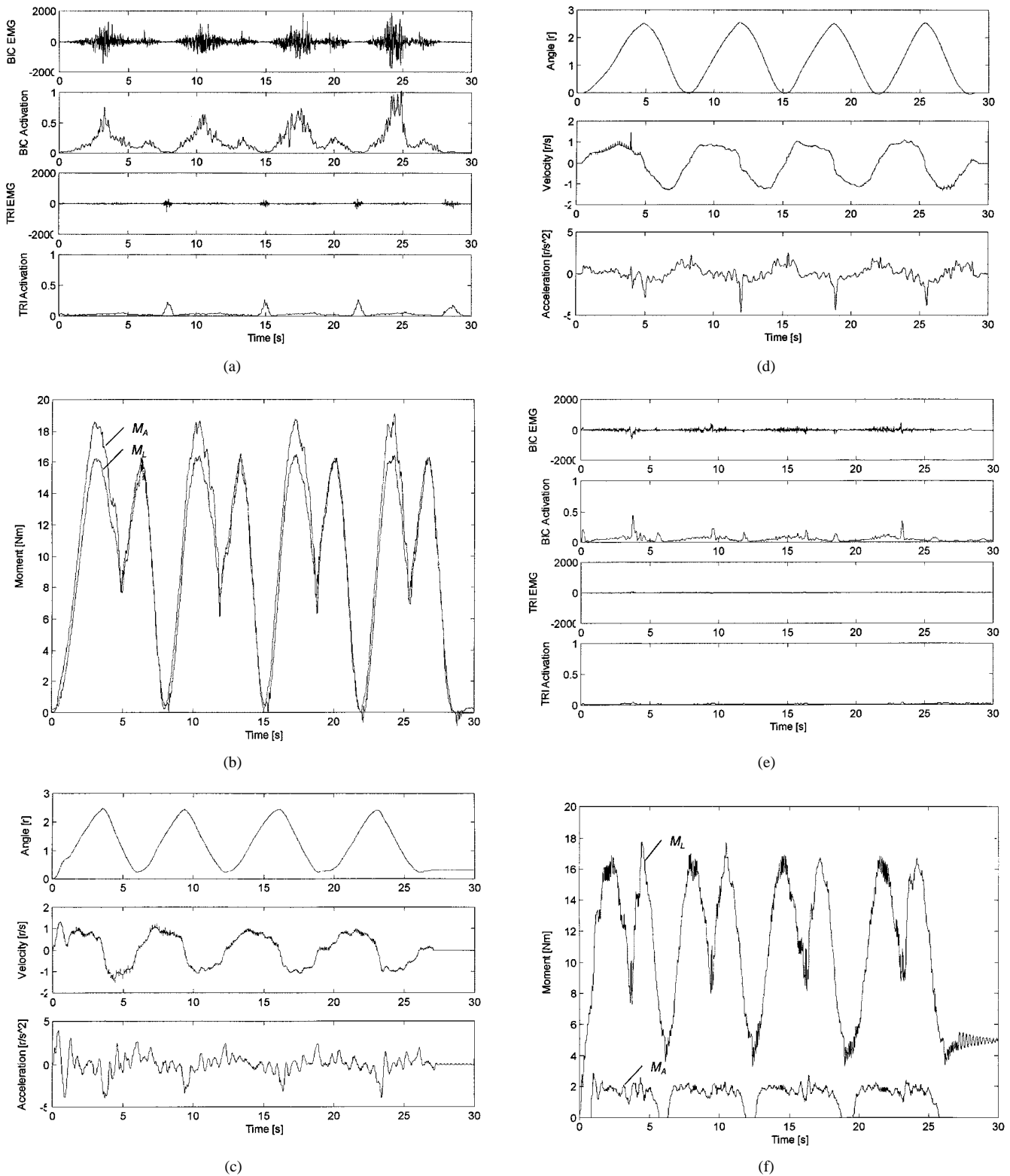
Fig. 6.   Exoskeleton performances in passive and active modes while maneuvering a weight. (a) EMG signal and muscle activation levels—passive mode (raw EMG signal in the range of ± 2000 represent the range of ± 2.5 mV, and the activation levels are dimensionless normalized EMG mV/mV). (b) Elbow joint kinematics—passive mode. (c) Moment relative to the elbow joint—passive mode. (d) EMG signals and muscle activation levels—active mode. (e) Elbow joint kinematics—active mode. (f) Moment relative to the elbow joint—active mode.

oskeleton actuator. The overall gain was 6, which means that the human carried 1/7 (14%) of the total load. The graphs denoted by G_{MA2}, G_{MA3}, G_{MA4}, G_{MA5}, and G_{MA6} were obtained by multiplying the graph denoted by G_{ME1} (experimental data)

by factors of 2, 3, 4, 5, and 6, respectively. This procedure defined five graphs representing artificially gained natural performance. As the gain increased, the graph became narrower since the overall gain was the tangent of the average graph slope. The
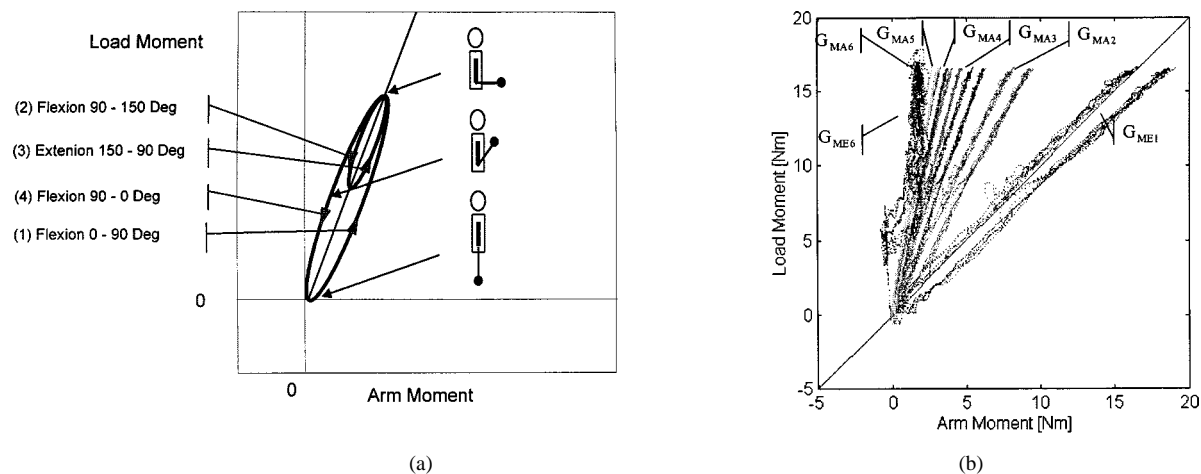
Fig. 7.   Moment index of performance (moment map)—load moment as a function of human arm moment during manipulating an object with the exoskeleton. (a) Schematic moment map. (b) Experimental results.

artificial gained data (G_{MA6}), which was referred as the target performance, was highly correlated with the experimental data (G_{ME6}) obtained by using the exoskeleton. This correlation indicated that the dynamical characteristics of a natural human arm movements were preserved during the exoskeleton operation, and in that way the exoskeleton may be considered as a natural extension of the human arm.

The gain mapping, including 93 experimental sessions, were analyzed according to the three indices of performance: mechanical moment gain (Section II-B—index ii, mechanical work ratio—Section II-B—index iii, and muscles' activation ratio Section II-B—index iv). The three diagrams are plotted for the three indices of performance using a three-dimensional (3-D) mesh (Figs. 8–10). The nonmeshed areas indicate nonstable exoskeleton operation and define the upper limit of the performance envelope.

The experimental data indicated that as the overall gain of the system increased (Fig. 8) both the mechanical work (Fig. 9) and the muscle activation (Fig. 10) decrease. Out of the three performance indices the mechanical moment gain index clearly indicated the advantage of using the EMG signals as a command signal (exoskeleton third generation). Using only the human arm and load moments (exoskeleton second generation) as a command signal, the maximal gain value was 8 (Fig. 8—0% normalized command gain—25% normalized feedback gain). Above that gain the system was not stable as indicated by the white nonmeshed area in Fig. 8 defining unstable operation. On the other hand, using only the EMG signals as a command the maximal gain value was 5.5 (Fig. 8—100% normalized command gain—0 normalized feedback gain). When the gains of the command signal (EMG) and the feedback signal (moment) were set to 40% and 100%, respectively, the overall mechanical gain increased to 16. Using the synthesis of EMG as a command signal, and moment signal as a feedback command, the exoskeleton gain performance was doubled.

IV. CONCLUSION

The level at which HMI is set for operating the exoskeleton system is a key element in determining the overall performance of the system, and the quality of its integration with the operator.
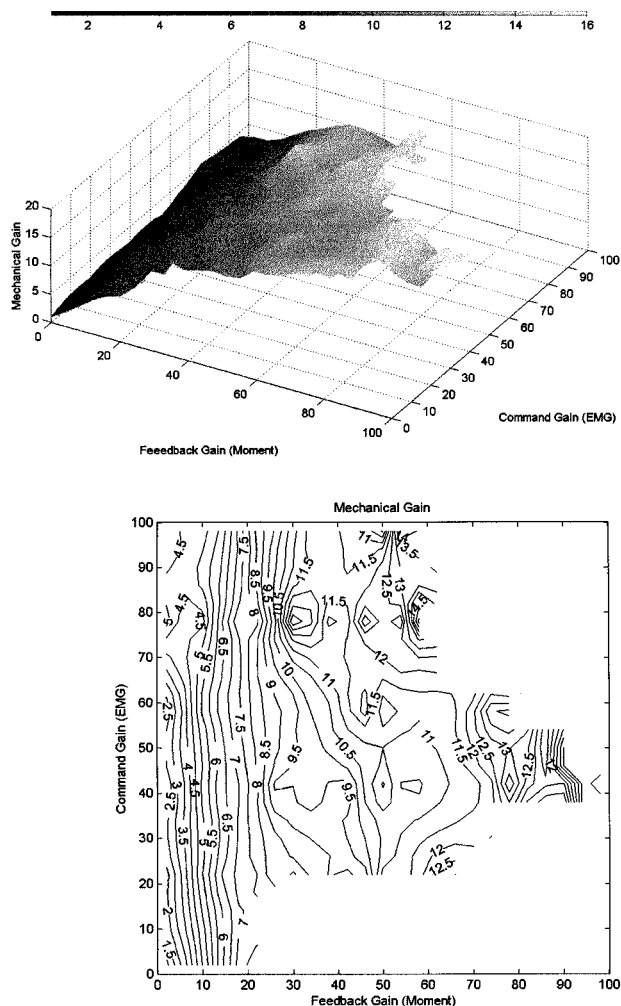

Fig. 8. Mechanical moment gain—index of performance.

This study proposes a new generation of exoskeletons by setting the interface at the human neuromuscular junction level, using myosignals (processed electromyography signals) as command signals for the exoskeleton system.

To evaluate this new exoskeleton concept, an experimental apparatus was built integrating hardware and software. While
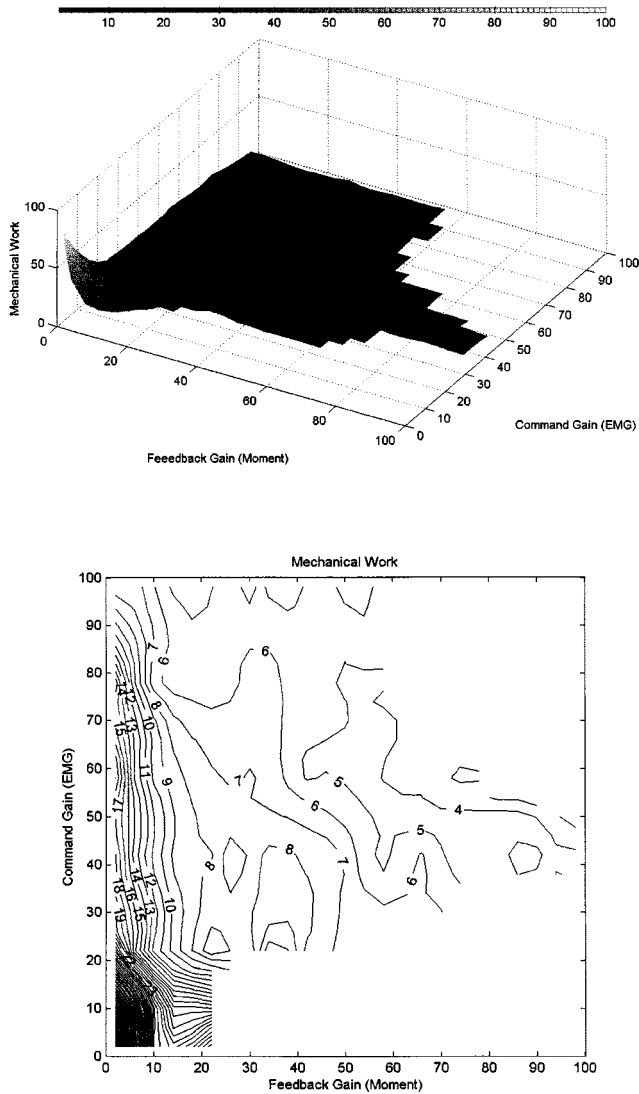
Fig. 9.   Mechanical work ratio—index of performance.

Fig. 10.   Muscle activation ratio—index of performance.

operating the system, the human had full contact with the device, sensing a scaled-down version of the external load. The deficiency of the myoprocessor moment prediction accuracy and the exoskeleton nonlinear dynamics was overcome by using a control algorithm with feedback loops based on the load/exoskeleton and human-arm/exoskeleton contact force.

The overall performance of the system was defined by four type of indices:

1) *moment index;*
2) *gain index;*
3) *work index;*
4) *muscle activation index.*

Synthesizing the processed EMG signals as command signals with load/human-arm moments feedback, improved the exoskeleton performance, as indicated by all the indices, compared to the exoskeleton performance achieved by using only one source of command signal. The mechanical gain increased from a value of 8 when using the moment command signal (second generation) to a value of 16, when synthesizing processed E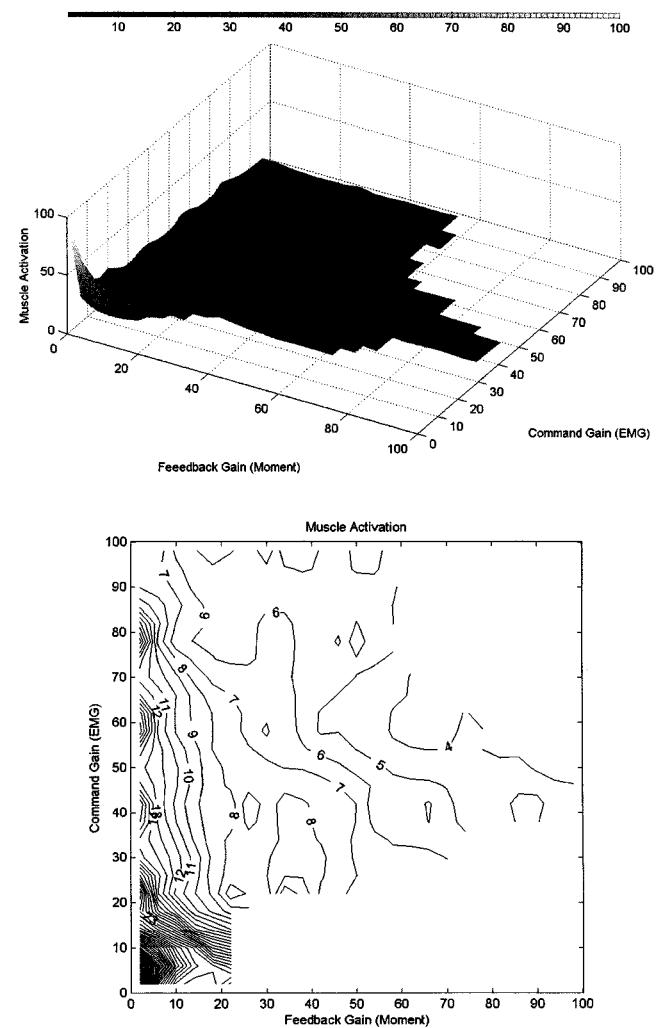MG command signals with the moment feedback signals (third generation). The mechanical gain increase was accompanied by a decrease in the muscle activation levels and reduction of the mechanical work. Improving the quality of the command signal further increased the overall mechanical gain of the exoskeleton system.

Two explanations were suggested for the overall performance enhancement using the EMG signals. The EMG signals most probably increased the significance of the command signal leading to improved signal-to-noise ratio (SNR). Improving this ratio allowed to further increase the overall mechanical gain of the exoskeleton system. In addition, from the theoretical point of view, gain and time delays are linked together. Inherent time delays in a system reduce the phase margin and hence the stability will be reduced [53]. By using the EMG signals in conjunction with the myoprocessor the system used parallel processing of the command signal as opposed to the second generation in which the physiological and the mechanical system were processing the command signal in a cascade fashion. Therefore, increasing the system gain is one of the leading advantages of the present concept.

This study evaluated the feasibility of a new exoskeleton system concept based on myosignals as command signals. Further research should focus on increasing the number of

joints to a full functional human arm exoskeleton (7 DOF). Further increase in the computational power of microprocessors will provide the ability to implement more advanced myoprocessors in a real-time mode and in that way to improve the muscle model moment prediction. Moreover, it will also allow to develop control algorithms based on neural network and fuzzy logic, which may be designed for specific operator. This will further improve the integration between human and machine as part of the quest of naturally controlled exoskeleton systems.

REFERENCES

[1] B. Hannaford, "Feeling is believing: Haptics and telerobotics technology," in *The Robot in the Garden: Telerobotics and Telepistemology in the Age of the Internet*, J. K. Goldberg, Ed. Cambridge, MA: MIT Press, 2000.
[2] S. C. Jacobsen, F. M. Smith, D. K. Backman, and E. K. Iversen, "High performance, high dexterity, force reflective teleoperator," in *Proc. 38th Conf. Remote Syst. Technol.*, Washington, DC, 1990, pp. 180–185.
[3] B. Hannaford and S. Venema, "Kinesthetic display for remote and virtual environment," in *Virtual Environment and Advanced Interface Design*, W. Barfield and T. A. Furness, Eds. Oxford, U.K.: Oxford Univ. Press, 1995, pp. 415–436.
[4] J. M. Hollerbach and S. C. Jacobsen, "Haptic interfaces for teleoperation and virtual environments," in *Proc. First Workshop Simulation Interaction Virtual Environments*, Iowa City, IA, 1995.
[5] G. C. Burdea, *Force and Touch Feedback for Virtual Reality*. New York: Wiley, 1996.
[6] B. M. Jau, "Anthropomorhic exoskeleton dual arm/hand telerobot controller," in *Proc. IEEE Int. Workshop Intelligent Robots*, Tokyo, Japan, 1988, pp. 715–718.
[7] F. P. Brooks, Jr., M. O. Young, J. J. Batter, and P. J. Kilpatrick, "Project GROPE-haptic displays for scientific visualization," *Comput. Graph.*, vol. 24, no. 4, pp. 177–185, Aug. 1990.
[8] M. Bergamasco, B. Allotta, L. Bosio, L. Ferretti, G. Parrini, G. M. Prisco, F. Salsedo, and G. Sartini, "An arm exoskeleton system for teleoperation and virtual environments applications," in *Proc. IEEE Int. Conf. Robotics Automat.*, vol. 2, San Diego, CA, 1994, pp. 1449–1454.
[9] D. G. Caldwell, O. Kocak, and U. Andersen, "Multi-armed dexterous manipulator operation using glove/exoskeleton control and sensory feedback," in *Proc. IEEE/RSJ Int. Conf. Intelligent Robots Syst.: Human Robot Interaction Cooperative Robots*, vol. 2, Pittsburgh, PA, 1995, pp. 567–572.
[10] D. W. Repperger, B. O. Hill, C. Hasser, M. Roark, and C. A. Phillips, "Human tracking studies involving an actively powered augmented exoskeleton," in *Proc. 15th Southern Biomed. Eng. Conf.*, Orlando, FL, 1996, pp. 28–31.
[11] Y. Umetani, Y. Yamada, T. Morizono, T. Yoshida, and S. Aoki, "'Skil mate' wearable exoskeleton robot systems," in *Proc. IEEE Int. Conf. Syst., Man, Cybern.*, vol. 4, Kyongju, Korea, 1999, pp. 984–988.
[12] L. Sooyong, L. Jangwook, C. Woojin, K. Munsang, L. Chong-Won, and P. Mignon, "A new exoskeleton-type masterarm with force reflection :controller and integration," in *Proc. IEEE/RSJ Int. Conf. Intelligent Robots Syst.*, vol. 3, 1999, pp. 1438–1443.
[13] L. Sooyong, L. Jangwook, C. Woojin, K. Munsang, and L. Chong-Won, "A new master-arm for man–machine interface," in *Proc. Syst., Man, Cybern. Conf.*, vol. 4, Tokyo, Japan, 1999, pp. 1038–1043.
[14] P. Brown, D. Jones, S. K. Singh, and J. M. Rosen, "The exoskeleton glove for control of paralyzed hands," in *Proc. IEEE Int. Conf. Robotics Automat.*, vol. 1, Atlanta, GA, 1993, pp. 642–647.
[15] B. M. Jau, "Dexterous telemanipulation with four fingered hand system," in *Proc. IEEE Int. Conf. Robotics Automat.*, vol. 1, Nagoya, Japan, 1995, pp. 338–343.
[16] R. S. Mosher, "Force reflecting electrohydraulic servo manipulator," *Electro-Tech.*, Dec. 1960.
[17] "Exoskeleton prototype project, final report phase I," General Electric Co., Schenectady, NY, Rep. S-67-1011, 1966.
[18] "Hardiman I prototype project, special interim study," General Electric Co., Schenectady, NY, Rep. S-68-1060, 1968.
[19] B. J. Makinson, "Research and development prototype for machine augmentation of human strength and endurance, Hardiman I project," General Electric Co., Schenectady, NY, Rep. S-71-106, 1971.
[20] P. Rabischong, "Robotics for the handicapped," in *Proc. IFAC Symp.*, Columbus, OH, May 1982.
[21] M. E. Rosheim, *Robot Evolution—The Development of Antrhrobotics*. New York: Wiley, 1994.
[22] H. Kazerooni and H. Ming-Gau, "The dynamics and control of a haptic interface device," *IEEE Trans. Robot. Automat.*, vol. 10, pp. 453–464, Aug. 1994.
[23] H. Kazerooni and T. J. Snyder, "Case study on haptic devices: Human-induced instability in powered hand controllers," *J. Guid. Contr. Dynam.*, vol. 18, no. 1, pp. 108–113, Jan./Feb. 1995.
[24] H. Kazerooni, "The human amplifier technology at the University of California, Berkeley," *Robot. Auton. Syst.*, vol. 19, pp. 179–187, 1996.
[25] T. J. Snyder and H. Kazerooni, "A novel material handling system," in *Proc. IEEE Int. Conf. Robotics Automat.*, Minneapolis, MN, Apr. 1996, pp. 1147–1152.
[26] E. A. Clancy and N. Hogan, "Single site electromyograph amplitude estimation," *IEEE Trans. Biomed. Eng.*, vol. 41, pp. 159–167, Feb. 1994.
[27] ——, "Influence of joint angle on the calibration and performance of EMG amplitude estimators," *IEEE Trans. Biomed. Eng.*, vol. 45, pp. 664–668, May 1998.
[28] ——, "Probability density of the surface electromyogram and its relation to amplitude detectors," *IEEE Trans. Biomed. Eng.*, vol. 46, pp. 730–739, June 1999.
[29] R. J. Triolo and G. D. Moskowitz, "The theoretical development of a multichannel time-series myoprocessor for simultaneous limb function detection and muscle force estimation," *IEEE Trans. Biomed. Eng.*, vol. 36, pp. 1004–1017, Oct. 1989.
[30] E. A. Clancy and N. Hogan, "Relating agonist–antagonist electromyograms to joint torque during isometric, quasiisotonic, nonfatiguing contractions," *IEEE Trans. Biomed. Eng.*, vol. 44, pp. 1024–1028, Oct. 1997.
[31] R. B. Jerard and S. C. Jacobsen, "A method for quantitatively relating skeletal joint torques to electromyographic signals (for prosthesis control theory)," in *Proc. 29th Annu. Conf. Eng. Med. Biol.*, Boston, MA, Nov. 1976, p. 298.
[32] C. J. Abul-Haj and N. Hogan, "Functional assessment of control systems for cybernetic elbow prostheses—II. Application of the technique," *IEEE Trans. Biomed. Eng.*, vol. 11, pp. 1037–1047, Nov. 1990.
[33] K. Kuribayashi, M. Takahashi, and T. Taniguchi, "An upper extremity prosthesis using SMA actuator," in *IEEE Proc. Int. Workshop Robot Commun.*, 1992, pp. 52–57.
[34] M. Zardoshti-Kermani, B. C. Wheeler, K. Badie, and R. M. Hashemi, "EMG feature evaluation for movement control of upper extremity prostheses," *IEEE Trans. Rehab. Eng.*, vol. 3, pp. 324–333, Dec. 1995.
[35] C. Bonivento and C. Fantuzzi, "Supervisory system of myoelectric prostheses," in *Proc. IEEE Int. Conf. Contr. Applicat.*, vol. 1, Trieste, Italy, 1998, pp. 61–65.
[36] W. S. Harwin, T. Rahman, and R. A. Foulds, "A review of design issues in rehabilitation robotics with reference to North American research," *IEEE Trans. Rehab. Eng.*, vol. 3, pp. 3–13, Mar. 1995.
[37] M. Soede, "Mental control load and acceptance of arm prosthesis," *Automedica*, vol. 4, pp. 183–191, 1982.
[38] D. Prutchi, "Relation between electrical and mechanical of muscle: The 3-D propagation pattern of motor unit action potentials," Ph.D. dissertation, Tel-Aviv Univ, Dept. Biomed. Eng., Israel, 1992.
[39] J. Rosen, M. B. Fuchs, and M. Arcan, "Performances of hill-type and neural network muscle models—Toward a myosignal based exoskeleton," *Comput. Biomed. Res.*, vol. 32, no. 5, pp. 415–439, Oct. 1999.
[40] J. V. Basmajian and R. Blumenstein, *Electrode Placement in EMG Biofeedback*. Baltimore, MD: Williams & Wilkins, 1980.
[41] P. J. Rasch, *Kinesiology and Applied Anatomy*. Philadelphia, PA: Lea & Febiger, 1989.
[42] J. V. Basmajian and C. J. Luca, *Muscle Alive*. Baltimore, MD: Williams & Wilkins, 1985.
[43] A. V. Hill, "The heat of shortening and the dynamic constants of muscle," *Proc. R. Soc. Lond. Biol.*, vol. 126, pp. 136–195, 1938.
[44] G. L. Zahalak, "Modeling muscle mechanics (and energetics)," in *Multiple Systems: Biomechanics and Movement Organization*, J. M. Winters and S. L.-Y. Woo, Eds. New York: Springer-Verlag, 1990, pp. 1–23.
[45] J. M. Winters and L. Stark, "Analysis of fundamental human movement patterns through the use of in-depth antagonistic muscle models," *IEEE Trans. Biomed. Eng.*, vol. BME-32, pp. 826–839, Oct. 1985.
[46] ——, "Task-specific second-order movement models are encompassed by a global eighth-order nonlinear musculo–skeletal model," in *Proc. IEEE Conf. Syst., Man, Cybern.*, AZ, Nov. 1985, pp. 1111–1115.

[47] J. M. Winters and A. M. Bagley, "Biomechanical modeling of muscle-joint system," *IEEE Eng. Med. Bio. Mag.*, vol. 7, pp. 17–21, Sept. 1987.

[48] J. M. Winters, "Hill-based muscle models: A systems engineering perspective," in *Multiple Systems: Biomechanics and Movement Organization*, J. M. Winters and S. L.-Y. Woo, Eds.   New York: Springer-Verlag, 1990, pp. 69–93.

[49] F. E. Zajac and J. M. Winter, "Modeling musculskeletal movement system: Joint and body segmental dynamics, musculoskeletal actuation, and neuromuscular control," in *Multiple Muscle System*, J. M. Winters and S. L. Y. Woo, Eds.   New York: Springer-Verlag, 1990, ch. 5.

[50] J. M. Winters and D. G. Kleweno, "Effect of internal upper-limb alignment on muscle contributions to isometric strength curves," *J. Biomech.*, vol. 26, no. 2, pp. 143–153, 1993.

[51] H. Hatze, *Myocybernetic Control Models of Skeletal Muscle*.   Pretoria, South Africa: Univ. South Africa Press, 1981.

[52] Kaufman *et al.*, "Physiological prediction of muscle forces—I. Theoretical formulation," *Neurosci.*, vol. 40, no. 3, pp. 781–792, 1991.

[53] G. F. Franklin, J. D. Powell, and M. L. Workman, *Digital Control of Dynamic Systems*, 3rd ed.   Reading, MA: Addison-Wesley, 1998.

Moshe Brand received the B.Sc and M.Sc. degrees in mechanical engineering from Tel-Aviv University, Isreal, in 1993 and 1997, respectively. He has been pursuing the Ph.D. degree since 1998.

From 1994 to 1998, he was a Research Engineer at the EMG-based powered exoskeleton study in the Department of Biomedical and Mechanics Engineering, Biomechanics Laboratory, Tel-Aviv University. His research interests include cardiovascular stent implants.

Moshe B. Fuchs received degrees in civil and aeronautical engineering from the Free University of Brussels (ULB), Belgium, and the Sc.D. degree in aerospace engineering from the Israel Institute of Technology, Haifa, in 1976.

He has also worked in the Israeli Aircraft Industry in structural analysis and fatigue. He joined Tel-Aviv University, Israel, in 1977, where he is currently an Associate Professor and Head of the Department of Solid Mechanics, Materials, and Systems. His fields of interest include structural optimization, intelligent structures, and biostructures.

Jacob Rosen received the B.Sc. degree in mechanical engineering and the M.Sc. and Ph.D. degrees in biomedical engineering, all from Tel-Aviv University, Isreal, in 1987, 1993, and 1997, respectively.

From 1987 to 1992, he served as an Officer in the Israel Defence Forces studying human–machine interfaces. From 1993 to 1997, he was a Research Associate developing and studying the EMG-based powered exoskeleton at the Department of Biomedical Engineering, Biomechanics Laboratory, Tel-Aviv University. During the same period of time he held a Biomechanical Engineering position in a startup company developing innovative orthopedic spine/pelvis implants. Since 1997, he has been at the University of Washington, Seattle, where he has been Research Assistant Professor of Electrical Engineering since 2000. His research interests focus on biomechanics, biorobotics, and human–machine interface.

Mircea Arcan received the D.Sc. degree in mechanics from the Polytechnical Institute of Timisoara, Romania, in 1963.

After an early career at the University of Bucharest, Romania, he joined Tel-Aviv University, Israel, in 1972, where he was a Professor of Experimental Mechanics at the Department of Solid Mechanics, Materials, and Systems, and a Professor of Biomechanics at the Department of Biomedical Engineering. The author of a textbook and a monograph, he published extensively in research journals and made significant contributions in experimental solid mechanics, contact problems, fracture mechanics, biomechanics, human body dynamics, and rehabilitation. He was also the Principal Investigator of the Exoskeleton project and was actively involved in scientific work until his very last days. He died on June 15, 2000.